Synthesis, Characterization, Antioxidant Activity, and DNA-Binding Studies of 1-Cyclohexyl-3-tosylurea and Its Nd(III), Eu(III) Complexes

Pin-Xian XI, Zhi-Hong XU, Xiao-Hui LIU, Feng-Juan CHEN, Liang HUANG, and Zheng-Zhi ZENG*

State Key Laboratory of Applied Organic Chemistry and College of Chemistry and Chemical Engineering, Lanzhou University; Lanzhou 730000, P. R. China.

Received December 10, 2007; accepted January 22, 2008; published online January 25, 2008

A new ligand, 1-cyclohexyl-3-tosylurea (H_2L), was prepared by condensation ethyl *N*-(3-tossulfonyl) carbamate and cyclohexanamine. Its two lanthanide(III) complexes, $Ln(H_2L)_3 \cdot 3NO_3$ [Ln=Nd (1), and Eu (2)], have been synthesized and characterized on the base of element analyses, ESI-MS, molar conductivities, IR spectra and thermogravimetry/differential thermal analysis (TG-DTA). In addition, the DNA-binding properties of the ligand and its complexes have been investigated by electronic absorption spectroscopy, fluorescence spectroscopy, circular dichroic (CD) spectroscopy and viscosity measurements. The experiment results suggest that the ligand and its two complexes bind to DNA *via* a groove binding mode, and the binding affinity of the complex 2 is higher than that of the complex 1 and the ligand. Furthermore, the antioxidant activity (superoxide and hydroxyl radical) of the ligand and its metal complexes was determined by using spectrophotometer methods *in vitro*. These complexes were found to possess potent antioxidant activity and be better than standard antioxidants like vitamin C and mannitol. In particular, complex 2 displayed excellent activity on the superoxide and hydroxyl radical.

Key words 1-cyclohexyl-3-tosylurea; rare earth complex; groove binding; antioxidant activity

The sulfonylureas have a wide range use in biology, and many of their ramifications have been used as anti-diabetic medicine and herbicide.[1,2] Sulfonylurea regulating biological functions of pancreatic islets, which has been used for the treatment of type 2 diabetes mellitus because of its insulin tropic activity on pancreatic islets.[3] Subsequent interests were focused on the redox properties, structures and biological activity of their transition metal complexes.[4] More recently, the lanthanide(III) complexes of sulfonylurea increasingly attracted attention, because of their certain anti-diabetic activities. Yet it is noticed that the DNA-binding investigation of such complexes have been done relatively few. Because the interaction between metal complexes and DNA is in close relationship with their potential biological and pharmaceutical activities,[5,6] studies on DNA-binding of metal complexes are very important in the development of new therapeutic reagents and DNA molecular probes. In order to find more effective and less toxic anti-diabetic drugs, thousands of analogues of sulfonlyureas were synthesized.[6,7] Here, we synthesized 1-cyclohexyl-3-tosylurea (H_2L) and its two lanthanide(III) complexes. In addition DNA-binding property of two lanthanide(III) complexes with 1-cyclohexyl-3-tosylurea is reported in this paper. These lanthanide compounds possibly represent a new class of potential anti-diabetic agent.

Experimental

Materials Nitroblue tetrazolium (NBT), methionine (MET), vitamin B_2 ($VitB_2$) were purchased from Sigma Chemical Co. Calf thymus DNA (CT-DNA) was purchased from Sigma without further purification. EDTA and Ln_2O_3 (Ln=Nd, Eu) were produced in China. All chemicals used were of analytical grade. The lanthanide(III) nitrates were prepared by dissolving Ln_2O_3 in HNO_3, and then crystallizing to get the products. All the experiments involving interaction of the ligand and the complexes with CT-DNA were carried out in doubly distilled water buffer containing 5 mM Tris[Tris(hydroxymethyl)-aminomethane] and 50 mM NaCl, and adjusted to pH 7.2 with hydrochloric acid. A solution of CT-DNA gave a ratio of UV absorbance at 260 and 280 nm of about 1.8—1.9, indicating that the CT-DNA was sufficiently free of protein.[8] The CT-DNA concentration per nucleotide was determined spectrophotometrically by employing an extinction coefficient of 6600 $M^{-1} cm^{-1}$ at 260 nm.[9] The ligand and the complexes were dissolved in a solvent mixture of 1% CH_3OH and 99% Tris–HCl buffer (5 mM Tris–HCl, 50 mM NaCl, pH 7.2) at concentration 1.0×10^{-5} M. An absorption titration experiment was performed by maintaining 10 μM compounds and varying the concentration of nucleic acid. While measuring the absorption spectra, an equal amount of CT-DNA was added to both the compound solution and the reference solution to eliminate the absorbance of CT-DNA itself. EDTA–Fe(II) and Na_2HPO_4–KH_2PO_4 buffers were prepared with twice distilled water.

Physical Measurements The melting points of the compounds were determined on a Beijing XT4-100x microscopic melting point apparatus (the thermometer was not corrected). Carbon, hydrogen, and nitrogen were analyzed on an Elemental Vario EL analyzer. The metal contents of the complexes were determined by titration with EDTA (xylenol orange tetrasodium salt used as an indicator and hexamethylidynetetraimine as buffer). Infrared spectra (4000—400 cm^{-1}) were determined with KBr disks on a Therrno Mattson FTIR spectrometer. The UV–visible spectra were recorded on a Varian Cary 100 UV–Vis spectrophotometer. The fluorescence spectra were recorded on a Hitachi RF-4500 spectrofluorophotometer. ^{1}H-NMR spectra were measured on a Varian VR 300-MHz spectrometer, using tetramethyl silicon (TMS) as a reference in dimethyl sulfoxide (DMSO)-d_6. The thermal behaviour was monitored on a PCT-2 differential thermal analyzer. Mass spectra were performed on a VG ZAB-HS (FAB) instrument and electrospray mass spectra (ESI-MS) were recorded on a LQC system (Finngan MAT, U.S.A.) using CH_3OH as mobile phase. All conductivity measurements were performed in *N*,*N*′-dimethyl formamide (DMF) with a DDS-11A conductor at 25 °C. The antioxidant activites were tested on a 721E spectrophotometer (Shanghai Analytical Instrument Factory, China).

Preparation of the Ligand (H_2L) The preparation of the ligand is shown in Fig. 1. A mixture of *p*-toluene sulfonamide (5.14 g, 0.03 mol) and finely pulverized K_2CO_3 (11.00 g, 0.078 mol) in 35 ml of acetone was stirred and heated to reflux for 30 min. Acetone solution (10 ml) of ethyl chloroformate (3.80 ml, 0.04 mol) was added to the refluxing mixture and heating continued for another 4 h. The mixture of the results were poured into 100 ml of H_2O, then the aqueous phase was acidified with 10 ml of 1.0 N aqueous HCl to get the solid, washed with 80 ml H_2O for several times. Recrystallization from 20 ml ethanol provided 6.35 g (87%) of ethyl *N*-(3-

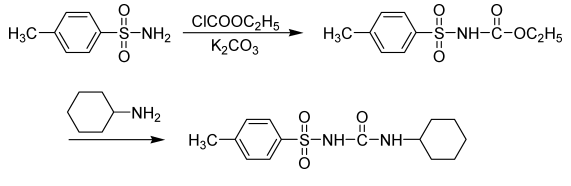

Fig. 1. The Preparation of the Ligand

* To whom correspondence should be addressed. e-mail: zengzhzh@yahoo.com.cn

toluenesulfonyl) carbamate as a white crystalline solid: mp 76—78 °C.

A solution of ethyl *N*-(3-toluenesulfonyl) carbamate (0.73 g, 3.00 mmol) and cyclohexanamine (0.45 ml, 3.90 mmol) in 40 ml PhMe was heated to reflux for 6 h. After the solution stood overnight at room temperature, the resulting precipitate was collected, washed twice time with PhMe, and dried in vacuum to afford 0.67 g (75%) of a white solid: mp 156—158 °C; H_2L (DMSO-d_6) δ (ppm): 0.96—1.86 (m, 10H), 2.31 (s, 3H), 2.89 (bm, 1H), 3.56 (bm, 1H), 7.16—7.19 (d, 2H, J=8.1 Hz), 7.59—7.62 (d, 2H, J=8.1 Hz). IR ν_{max} (cm^{-1}): ν_{NH} (CONH): 3340, ν_{NH} (SOONH): 3047, ν (C=O): 1704, ν (S=O): 1130. U_{max}: (CH_3OH) nm (log ε) 205 (4.61), 227(4.66). FAB-MS: m/z=297 $[M+H]^+$. *Anal.* Calcd for $C_{14}H_{20}N_2O_3S$: C, 56.73; H, 6.80; N, 9.45. Found: C, 56.80; H, 6.75; N, 9.56.

Preparation of the Complexes The complex **1** was prepared as follows. The solution of $Nd(NO_3)_3\cdot 6H_2O$ (438.25 mg, 1 mmol) in anhydrous methanol (10 ml) was added dropwise to the solution of the ligand (296.38 mg, 1 mmol) in warm (60 °C) anhydrous methanol (10 ml) with stirring magnetically over 2 h. The clear solution obtained was reduced under vacuum to 8 ml, water (40 ml) was added to the residue with stirring magnetically and the resulting solid was collected by filtration. The product was recrystallized from mixture solvent of methanol and water (1 : 3), and dried in a vacuum desiccator. Yield: 75%. The complex **2** was synthesized by the same way. *Anal.* Calcd for complex **1** $C_{42}H_{60}N_9O_{18}S_3Nd$: C, 41.37; H, 4.96; N, 10.34; Nd, 11.83. Found: C, 41.41; H, 4.90; N, 10.31; Nd, 11.89. Λ_m ($s\,cm^2\,mol^{-1}$): 21.7. ESI-MS [CH_3OH, m/z]: 1217.2 ($\{[Nd(H_2L)_3\cdot 3NO_3]+H\}^+$), 1154.3 ($\{[Nd(H_2L)_3\cdot 3NO_3]-NO_3\}^+$), 1091.3 ($\{[Nd(H_2L)_3\cdot 3NO_3]-2NO_3-H\}^+$), IR ν_{max} (cm^{-1}): $\nu_{(aminoantipyrine)}$ (C=O): 1700 cm^{-1}, $\nu_{(carbonyl)}$ (C=O): 1615 cm^{-1}, $\nu_{(-SOONH-)}$ (N–H): 3727 cm^{-1}, ν (NO_3): 1479, 840. U_{max}: (CH_3OH) nm (log ε): 206 (4.61), 228 (4.66), 272 (4.74). *Anal.* Calcd for complex **2** $C_{42}H_{60}N_9O_{18}S_3Eu$: C, 41.11; H, 4.93; N, 10.27; Eu, 12.38. Found: C, 41.16; H, 4.86; N, 10.23; Eu, 12.30. Λ_m ($s\,cm^2\,mol^{-1}$): 33.6. ESI-MS [CH_3OH, m/z]: 1227.2 ($\{[Eu(H_2L)_3\cdot 3NO_3]+H\}^+$), 1165.3 ($\{[Eu(H_2L)_3\cdot 3NO_3]-NO_3\}^+$), 1102.3 ($\{[Eu(H_2L)_3\cdot 3NO_3]-2NO_3-H\}^+$); IR ν_{max} (cm^{-1}): $\nu_{(aminoantipyrine)}$ (C=O): 1700 cm^{-1}, $\nu_{(carbonyl)}$ (C=O): 1615 cm^{-1}, $\nu_{(-SOONH-)}$ (N–H): 3727 cm^{-1}, ν (NO_3): 1479, 840. U_{max}: (CH_3OH) nm (log ε) 206 (4.61), 228 (4.66), 272 (4.74).

Superoxide Radical Scavenging Assay The superoxide radicals ($O_2^{-\cdot}$) were generated *in vitro* by non-enzymatic system and determined spectrophotometrically by NBT photoreduction method with a little modification in the method adopted elsewhere.[10—13] The amount of $O_2^{-\cdot}$ and suppression ratio for $O_2^{-\cdot}$ can be calculated by measuring the absorbance at 560 nm. Solution of MET, $VitB_2$ and NBT were prepared at avoiding light. The tested compounds were dissolved in DMF. The assay mixture, in a total volume of 5 ml, contained MET (10 mM), NBT (46 μM), $VitB_2$ (3.3 μM), the tested compound (10—30 μM) and a phosphate buffer (67 mM, pH 7.8). After illuminating with a fluorescent lamp at 30 °C for 10 min, the absorbance of the samples (A_i) was measured at 560 nm. The sample without the tested compound was used as control and its absorbance was A_0. All experimental results were expressed as the mean±standard deviation (S.D.) of triplicate determinations. The suppression ratio for $O_2^{-\cdot}$ was calculated from the following expression:

$$\text{suppression ratio (\%)} = A_0 - A_i/A_0 \times 100 \quad (1)$$

Drug activity was expressed as the 50% inhibitory concentration (IC_{50}). IC_{50} values were calculated from regression lines where: x was the tested compound concentration in mM and y was percent inhibition of the tested compounds.

Hydroxyl Radical Scavenging Assay The hydroxyl radicals ($OH^{\cdot}$) in aqueous media were generated through the Fenton system.[14] The solution of the tested compound was prepared with DMF. The 5 ml assay mixture contained following reagents: safranin (11.4 μM), EDTA–Fe(II) (40 μM), H_2O_2 (1.76 mM), the tested compound (10—30 μM) and a phosphate buffer (67 mM, pH 7.4). The assay mixtures were incubated at 37 °C for 30 min in a waterbath. After which, the absorbance was measured at 520 nm. All the tests were run in triplicate and expressed as the mean±standard deviation (S.D.).

The suppression ratio for $OH^{\cdot}$ was calculated from the following expression:

$$\text{suppression ratio (\%)} = [(A_i - A_0)/(A_c - A_0)] \times 100 \quad (2)$$

(Where A_i=the absorbance in the presence of the tested compound; A_0=the absorbance in the absence of the tested compound; A_c=the absorbance in the absence of the tested compound, EDTA–Fe(II), H_2O_2.)

Results and Discussion

All of the complexes are air stable for extended periods and soluble in DMSO (dimethylsulphoxide) and DMF; slightly soluble in methanol and ethanol; insoluble in benzene, water and diethyl ether. The molar conductivities in DMF solution indicate that the complex **1** and complex **2** (21.7, 33.6 $s\,cm^2\,mol^{-1}$) are in the range expected for no electrolytes.[15] The elemental analyses, ESI-MS and molar conductivities show that the formulas of the complexes conform to $Ln(H_2L)_3\cdot 3NO_3$ [where Ln=Nd(III) and Eu(III)].

IR Spectra The IR spectra of the complexes are similar. The band of ν (C=O) appeared at 1704 cm^{-1} in the ligand while the band of the complexes was exhibited at 1641 cm^{-1}; $\Delta\nu_{(ligand\text{-}complexes)}$ is equal to 63 cm^{-1}. This shift confirms that the group loses its original characteristics and forms coordinative bonds with the metal.[16] The band at the 1130 cm^{-1} was ν (S=O) vibration in the ligand. In the complexes these bands are presented at 1090 cm^{-1}. $\Delta\nu_{(ligand\text{-}complexes)}$ is equal to 40 cm^{-1}. The spectra of the ligand exhibit ν_{NH} (CONH) vibration bands at the 3340 cm^{-1} and ν_{NH} (SOONH) vibrations at the 3047 cm^{-1}, in the complexes the ν_{NH} (CONH) and the ν_{NH} (SOONH) vibration were blue shifted to 3473 cm^{-1} and 3278 cm^{-1} respectively. In the complexes, the band at 560 cm^{-1} or so is assigned to ν (Ln–O). These shifts demonstrate that the ligand coordinated Nd^{3+} and Eu^{3+} ions through the oxygen of carbonyl and sulphanilamide. Weak bands at 425 cm^{-1} are assigned to ν (Ln–N). These shifts and the new band further confirm that the nitrogen of the imino-group bonds to the rare earth ions. The absorption bands of the coordinated nitrates were observed at about 1479 (ν_{as}) and 840 (ν_s) cm^{-1}.[17]

UV Spectra The study of the electronic spectra in the ultraviolet and visible ranges for the complexes and the ligand were carried out in a solvent mixture of 1% CH_3OH and 99% Tris–HCl buffer. The electronic spectra of ligand had a strong band at λ_{max}=203 nm, a medium band at λ_{max}=227 nm. The complexes also yield two bands at about 207 and 231. A new band appeared at 275 nm for complex **1** and **2**. These changes indicate that complexes are formed.

Thermal Analyses Some data of thermal analyses are listed in Table 1. The DTA curves of the complexes have an endothermic peak between 90 and 96 °C, the corresponding TG curves show that the weight loss is equal to around three water molecules. These results are in accordance with the

Table 1. Thermal Analyses Data of the Complexes

Complex	D[a] T°C	Process	%H_2O loss		Decomposed			Process	Residue
			Calc.	Found	T1	T2	T3		
1	96	Endothermic	4.98	5.21	341	453	556	Exothermic	Nd_2O_3
2	90	Endothermic	4.94	5.17	337	448	538	Exothermic	Eu_2O_3

compositions of the complex determined by elemental analyses. Exothermic peaks appear around 331—363, 445—458 and 536—558 °C, respectively. Initial temperature decomposed is greater than 330 °C, this indicates that thermal stability of the complexes are higher than that of the free ligand, whose stability shows that there may be a large conjugation chelate ring exists in the complex.

Since the crystal structures of the complexes have not been obtained yet, we characterized the complexes and determined their possible structure by elemental analyses, ESI-MS, molar conductivities, IR data, TG-DTA, and UV–vis measurements. The likely structure of the complexes is shown in Fig. 2.

DNA-Binding Studies. Electronic Absorption Titration Electronic absorption spectroscopy is universally employed to determine the binding characteristics of metal complex with DNA.[18] The absorption spectra of the ligand, complex **1** and complex **2** in the absence and presence of CT-DNA are given in Figs. 3a, b and c, respectively. There exist in Fig. 3a two well-resolved bands at about 202 and 230 nm for the ligand, and in Figs. 3b and c also have two well-resolved bands at about 204 and 230 nm for the complexes. With increasing DNA concentrations, the hypochromisms increased up to 9.20% at 202 nm and 8.13% at 230 nm for ligand; 35.40% at 203 nm and 8.10% at 230 nm for complex **1**; 51.61% at 204 nm and 32.46% at 230 nm for complex **2**. The λ_{max} for the ligand increased from 202 to 203, for complex **1** increased from 203 to 205 nm and that for complex **2** increased from 204 to 206 nm. Such a small change in λ_{max} is more in keeping with groove binding, leading to small perturbations. Such small increases in the λ_{max} and the hypochromicity have been observed in the case of some porphyrin and copper complexes on their interaction with DNA.[19,20]

The absorption data were analyzed to evaluate the intrinsic binding constant K_b, which can be determined from Eq. 3[21]

$$[DNA]/(\varepsilon_a-\varepsilon_f)=[DNA]/(\varepsilon_b-\varepsilon_f)+1/K_b(\varepsilon_b-\varepsilon_f) \quad (3)$$

where [DNA] is the concentration of DNA in base pairs, the apparent absorption coefficient ε_a, ε_f and ε_b correspond to A_{obsd}/[M], the extinction coefficient of the free compound and the extinction coefficient of the compound when fully bound to DNA, respectively. The binding constants, K_b for the complexes **1** and **2** have been determined from the plot of [DNA]/($\varepsilon_a-\varepsilon_f$) *vs.* [DNA] and found to be 2.6×10^4 M^{-1} and 7.8×10^4 respectively, and the K_b for the ligand (0.31×10^4 M^{-1}) is very small. The K_b value obtained here is lower than that reported for classical intercalator (for ethidium bromide and [Ru(phen)DPPZ] whose binding constants have been found to be in the order of 10^6—10^7 M).[22,23] The

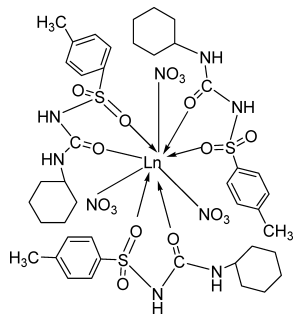

Fig. 2. The Suggested Structure of the Complexes

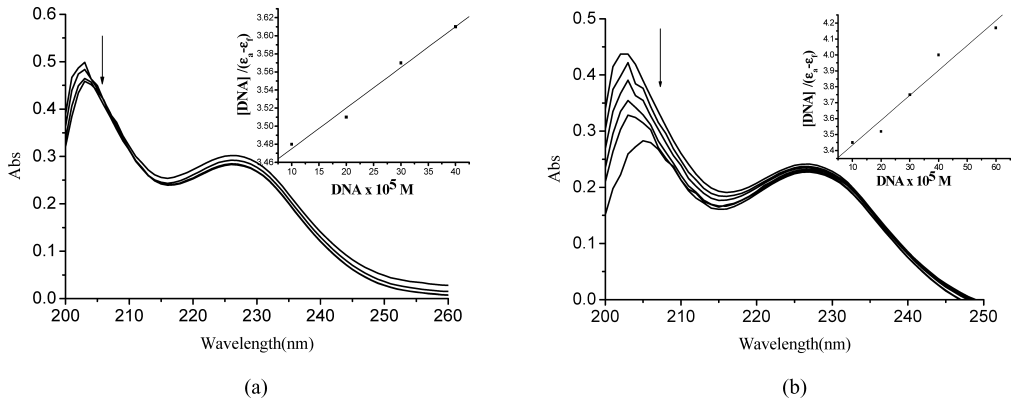

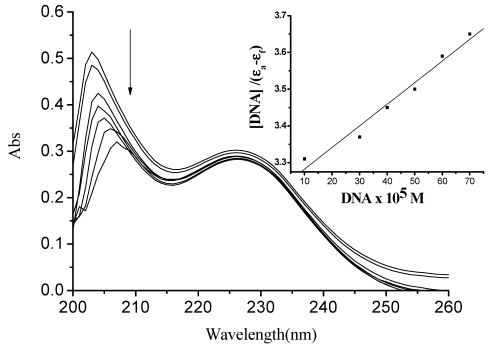

Fig. 3. Electronic Spectra of the Ligand (a), Complex **1** (b), Complex **2** (c) (10 μM) in the Presence of 0—70 μl 1.0×10^{-3} M CT-DNA

Arrow shows the emission intensities changes upon increasing DNA concentration. Inset: plots of [DNA]/($\varepsilon_a-\varepsilon_f$) *vs.* [DNA] for the titration of compound.

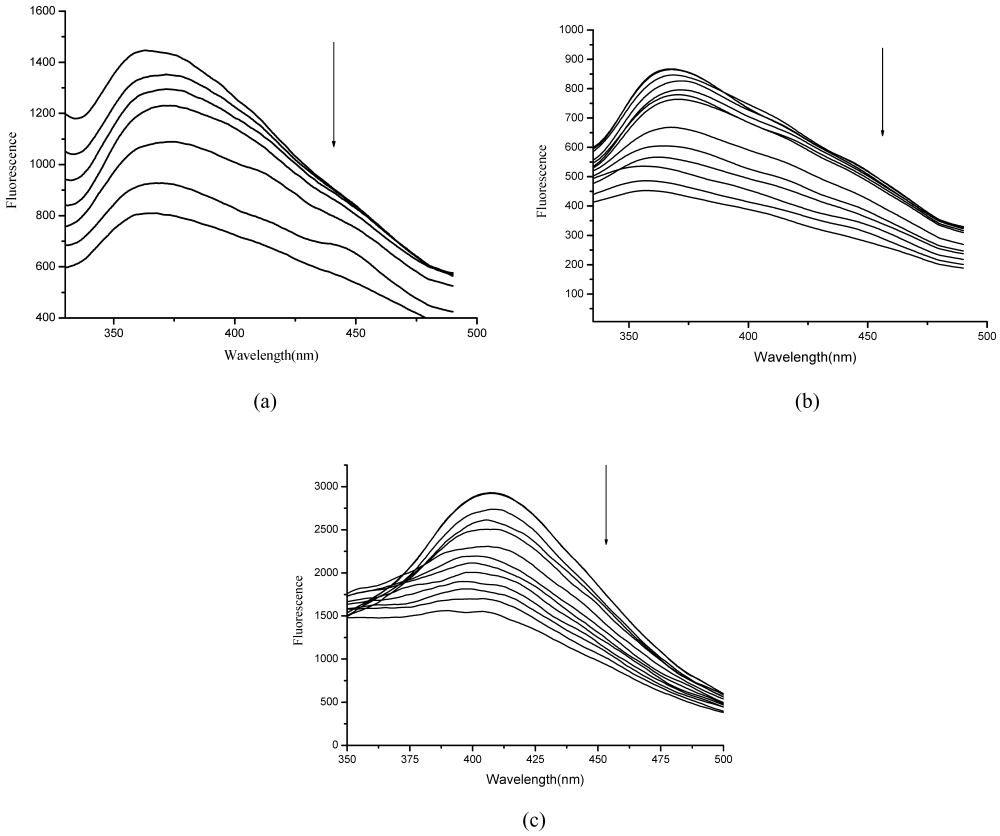

Fig. 4. The Emission Enhancement Spectra of the Ligand (a), Complex **1** (b), Complex **2** (c) (10 μM) in the Presence of 0—100 μl 1.0×10^{-3} M CT-DNA
Arrow shows the emission intensities changes upon increasing DNA concentration.

observed binding constant is more in keeping with the groove binding with DNA, as observed in the literature.[24,25] The results indicate that the binding strength of complex **2** is stronger than that of **1** and the ligand.

Fluorescence Spectra Fixed amounts (10 μM) of the complexes were titrated with increasing amounts of CT-DNA. Excitation and emission wavelengths of the samples were 256 and 370 nm, slit width 5/10 nm. All experiments were conducted at 20 °C in a solvent mixture of 1% CH_3OH and 99% Tris–HCl buffer.

The ligand and complexes emit luminescence in Tris buffer with a maximum appearing at 375 nm. The fluorescence titrations spectra of the ligand, complex **1** and complex **2** in the absence and presence of CT-DNA are given in Figs. 4a, b and c. Compared to the ligand and complexes alone, the fluorescence intensity decrease with the increase of CT-DNA concentration. As shown in Fig. 4, the fluorescence intensity of the complex **1** and **2** are quenched steadily with the increasing concentration of the CT-DNA. This phenomenon of the quenching of luminescence of the complex by DNA may be attributed to the photoelectron transfer from the guanine base of DNA to the excited metal-to-ligand charge transfer (MLCT) state of the complex.[24,26—31]

Circular Dichroic (CD) Spectroscopy CD spectral variations of CT-DNA were recorded by the respective addition of the ligand and complex **1** and **2** to CT-DNA. Figure 5 shows the CD spectra of CT-DNA which was added with the ligand, complex **1** and **2**. The observed CD spectrum of calf thymus DNA consists of a positive band at 277 nm due to base stacking and a negative band at 245 nm due to helicity,

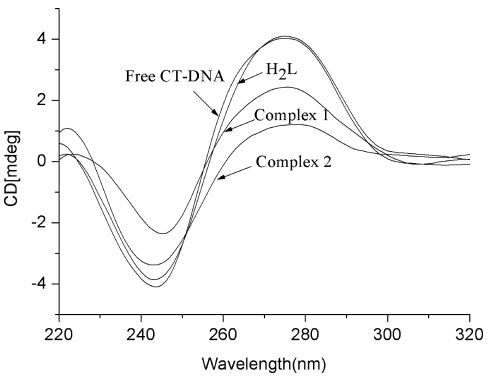

Fig. 5. CD Spectrum of CT-DNA Adduct with Compound
r_i=molar ratio, compound: CT-DNA.

which is characteristic of DNA in the right-handed B form. While groove binding interaction of small molecules with DNA show little or no perturbations on the base stacking and helicity bands, intercalation enhances the intensities of both the bands, stabilizing the right-handed B conformation of CT-DNA. In all two cases, the intensities of both the negative and positive bands decrease significantly. This suggests that the DNA binding of the complexes induces certain conformational changes, such as the conversion from a more B-like to a more C-like structure within the DNA molecule.[32] These changes are indicative of a non-intercalative mode of binding of these complexes and offer support to their groove binding nature.[33,34]

Viscosity Studies Hydrodynamic measurements that are

sensitive to the length change (*i.e.*, viscosity and sedimentation) are regarded as the least ambiguous and the most critical tests of a binding model in solution in the absence of crystallographic structural data.[8,35] As a means for further clarifying the binding of these compounds with DNA, viscosity studies were carried out. Data are presented as $(\eta/\eta_0)^{1/3}$ *versus* $1/R$, where R=[DNA]/[compound]; η and η_0 are the relative viscosities of DNA in the presence and absence of compound, respectively. The relative viscosity values were calculated from the flow time of DNA-containing solution (t) and the flow time of buffer alone (t_0), using the following expression[36]:

$$\eta=(t-t_0)/t_0 \quad (4)$$

Intercalating agents are expected to elongate the double helix to accommodate the ligands in between the base leading to an increase in the viscosity of DNA. In contrast, complexes that bind exclusively in the DNA grooves by partial and/or non-classical intercalation, under the same conditions, typically cause less pronounced (positive or negative) or no change in DNA solution viscosity.[37] Figure 6 shows the relative viscosity of DNA (50 μM) in the presence of varying amounts of the ligand, complexes **1** and **2**. The results reveal that the complexes **1** and **2** show relatively small changes in DNA viscosity, indicating that they bind weakly to DNA which is consistent with DNA groove binding suggested above.[38,39] The increased degree of viscosity, which may depend on its affinity to DNA follows the order of **2**>**1**>ligand, which is consistent with our foregoing hypothesis.

Antioxidant Activity It can be seen that the inhibitory effect of the tested complexes on $O_2^{-\cdot}$ are concentration related and the suppression ratio increases with the increasing of sample concentration in the range of the tested concentration (Fig. 7). The antioxidant activities of these compounds are expressed as 50% inhibitory concentration (IC_{50} in μM). IC_{50} values of **1** and **2** are 9.81±0.87 and 14.36±0.68 μM, respectively. Although the IC_{50} value of the ligand can not be read in Fig. 7, the compound **1** shows better inhibitory effect than **2** and the ligand.

We can find that all compounds scavenge $OH^{\cdot}$ also in a concentration-dependent manner. The complexes show highly active scavenging effect on $OH^{\cdot}$. Moreover, mannitol is a well-known natural antioxidant, so we also studied the scavenging activity of mannitol against hydroxyl radical using the same model. We find that when arriving at similar suppression ratio, concentration of the two complexes is far less than that of mannitol. The suppression ratio take the order of **1**>**2**>ligand.

It is clear that the scavenger effect on $O_2^{-\cdot}$ can be enhanced by the formation of metal-ligand coordination complexes and the nature of the rare earth ions also affects the ability. Some complexes are better effective inhibitor for $O_2^{-\cdot}$ than that of the nitroxide Tempo (IC_{50}=60±3.10 μM) which has been recently used in biological system for its capacity to mimic superoxide dismutase.[40] Although superoxide is a relatively weak oxidant, it decomposes to form stronger relative oxidative species, such as single oxygen and hydroxyl radicals, which initiate peroxidation of lipids.[41] In the present study, the complexes effectively scavenged superoxide in a concentration-dependent manner. These results showed the complexes have significant scavenging activity of superoxide radical and clearly suggested that the antioxidant activity of the complexes was also related to its ability to scavenge superoxide radical.

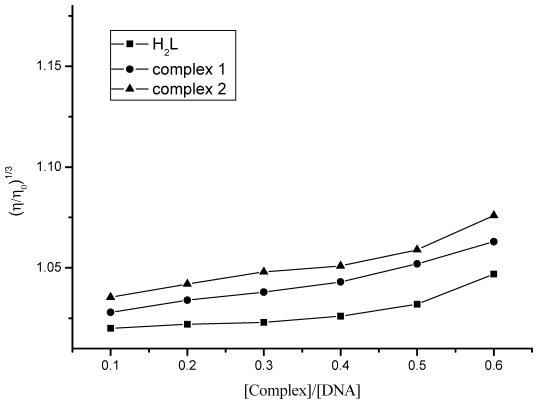

Fig. 6. Effect of Increasing Amounts of the Complexes on the Relative Viscosity of CT-DNA at 25.0±0.1 °C

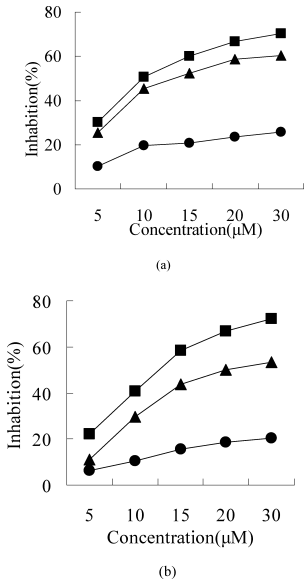

Fig. 7. (a) Effect of Tested Compounds on $O_2^{-\cdot}$ and (b) Effect of Tested Compounds on $OH^{\cdot}$

●, (ligand); ▲, (complex **1**); ■, (complex **2**); experiments were performed in triplicate. Values are expressed as mean±standard deviation (n=3).

It is clearly shown that metal complexes exhibit considerable scavenging activity due to the chelation of organic molecule to rare earth ions and rare earth ions such as La(III), Sm(III), Eu(III) and Dy(III) exert differential and selective effects on scavenging radicals of the biological system. Moreover, we find that the two complexes are better effective inhibitor for $OH^{\cdot}$ than that of mannitol which is usually used as special scavenger for $OH^{\cdot}$. Therefore, the metal complexes we studied in this paper deserve to be further researched.

Conclusion

In this paper, we have investigated and characterized H_2L and its two lanthanide(III) complexes $Ln(H_2L)_3\cdot 3NO_3$ [Ln=Nd (**1**), and Eu (**2**)]. In addition, the DNA-binding properties were investigated by electronic absorption, fluorescence, CD spectroscopy and viscosity measurement. The results support the fact that complex **1**, **2** and the ligand can

bond to CT-DNA by the mode of groove binding, and complex **2** has stronger binding affinity than **1** and the ligand. Furthermore, the two rare earth complexes have active scavenging effect on $O_2^{-\cdot}$ and $OH^{\cdot}$. According to the IC_{50} values obtained, complex **2** was found to exert superior activity in comparison to the remaining compounds. These findings clearly indicate that lanthanide-based complexes have many potential practical applications, like the development of nucleic acid molecular probes and new therapeutic reagents for diseases.

Acknowledgment This project was supported by the National Natural Science Foundation in China (20171019) and Zhide Foundation.

References

1) Howbert J. J., Grossman C. S., Crowell T. A., Rieder B. J., *J. Med. Chem.*, **33**, 2393—2407 (1990).
2) Williams D. R., *Chem. Rev.*, **72**, 203—213 (1972).
3) Groop L. C., *Diabetes Care*, **15**, 737—754 (1992).
4) Kessissoglou D. P., Manoussakis G. E., Hatzidimitriou A. G., Kanatzidis M. G., *Inorg. Chem.*, **26**, 1395—1402 (1987).
5) Xu H., Liang Y., Zhang P., Pu F., Zhou B. R., Wu J., Liu J. H., Liu Z. G., Ji L. N., *J. Biol. Inorg. Chem.*, **10**, 529—538 (2005).
6) Song Y. M., Wu Q., *J. Inorg. Biochem.*, **100**, 1685—1691 (2006).
7) Xu H., Zheng K. C., Deng H., Lin L. J., Zhang Q. L., Ji L. N., *Dalton Trans.*, **3**, 2260—2268 (2003).
8) Marmur J., *J. Mol. Biol.*, **3**, 208—218 (1961).
9) Kumar C. V., Asuncion E. H., *J. Am. Chem. Soc.*, **115**, 8547—8553 (1993).
10) Marta G. A., Gloria A., Joaquín B., Lucas D. C. A., Santiago G. G., José M. M. B., *Inorg. Chem.*, **44**, 9424—9433 (2005).
11) Winterbourn C. C., *Biochem. J.*, **182**, 625—628 (1979).
12) Sharma S. D., Rajor H. K., Chopra S., Sharma R. K., *BioMetals*, **18**, 143—154 (2005).
13) Li T. R., Yang Z. Y., Wang B. D., *Chem. Pharm. Bull.*, **55**, 26—28 (2007).
14) Winterbourn C. C., *Biochem. J.*, **198**, 125—131 (1981).
15) Geary W. J., *Coord. Chem. Rev.*, **7**, 81—122 (1971).
16) Zeng Y. B., Tang N., *J. Inorg. Biochem.*, **97**, 258—264 (2003).
17) Nakamato K., "Infrared and Raman Spectra of Inorganic and Coordination Compound," 3rd ed., Wiley-Interscience, New York, 1978.
18) Li H., Le X. Y., Pang D. W., Deng H., Xu Z. H., Lin Z. H., *J. Inorg. Biochem.*, **99**, 2240—2247 (2005).
19) Pasternack R. F., Gibbs E. J., Villafranca J. J., *Biochem. J.*, **22**, 2406—2414 (1983).
20) Vaidyanathan V. G., Nair B. U., *Eur. J. Inorg. Chem.*, **2004**, 1840—1846 (2004).
21) Wolf A., Shimer G. H., Meehan T., *Biochem. J.*, **26**, 6392—6396 (1987).
22) Cory M., McKee D. D., Kagan J., Henry D. W., Miller J. A., *J. Am. Chem. Soc.*, **107**, 2528—2536 (1985).
23) Waring M. J., *J. Mol. Biol.*, **13**, 269—282 (1965).
24) Vaidyanathan V. G., Nair B. U., *J. Inorg. Biochem.*, **94**, 121—126 (2003).
25) Vijayalakshmi R., Unni Nair B., *Biochim. Biophys. Acta*, **1475**, 157—162 (2000).
26) Xu Z. H., Chen F. J., Xi P. X., Liu X. H., Zeng Z. Z., *J. Photochem. Photobiol. A: Chem.* (2007), doi:10.1016/j.jphotochem.2007.11.017
27) Mesmaeker A. K., Orellana G., Barton J. K., Turro N. J., *J. Photochem. Photobiol.*, **52**, 461—472 (1990).
28) Chaires J. B., Dattagupta N., Crothers D. M., *Biochem. J.*, **21**, 3933—3940 (1982).
29) Wu J. Z., Yuan L., Wu J. F., *J. Inorg. Biochem.*, **99**, 2211—2216 (2005).
30) Xi P. X., Liu X. H., Lu H. L., Zeng Z. Z., *Transition Met. Chem.*, **32**, 757—761 (2007).
31) Peng B., Chao H., Sun B., Li H., Gao F., Ji L. N., *J. Inorg. Biochem.*, **101**, 404—411 (2007).
32) Mahadevan S., Palaniandavar M., *Inorg. Chem.*, **37**, 693—700 (1998).
33) Maheswari P. U., Palaniandavar M., *J. Inorg. Biochem.*, **98**, 219—230 (2004).
34) Zhang Z., Qian X. H., *Int. J. Biol. Macromol.*, **38**, 59—64 (2006).
35) Satyanarayana S., Dabrowiak J. C., Chaires J. B., *Biochem. J.*, **31**, 9319—9324 (1992).
36) Cohen G., Eisenberg H., *Biopolymers*, **8**, 45—55 (1969).
37) Liu C. S., Zhang H., Chen R., Shi X. S., Bu X. H., Yang M., *Chem. Pharm. Bull.*, **55**, 996—1001 (2007).
38) Lerman L., *J. Mol. Biol.*, **3**, 18—30 (1961).
39) Mahadevan S., Palaniandavar M., *Inorg. Chim. Acta*, **254**, 291—302 (1997).
40) Samuni A., Krisna M. C., "Handbook of Synthetic Antioxidants," ed. by Packer L., Cadenas E., Marcel Dekker, New York, 1997, pp. 351—373.
41) Zhong Z. M., Xing R. G., Liu S., Li P. C., *Eur. J. Med. Chem*., (2007). doi:10.1016/j.ejmech.2007.10.018.